



Fault identification approach and its application for predicting coal and gas outbursts

Ying Chen^{1,2,3} · Fenghua Xie¹ · Xiufeng Zhang⁴ · Cunwen Wang⁴ · Xiaotian Xu^{3,5} · Xiudong Wang^{3,5} · Yu Wang^{3,6}

Received: 29 September 2020 / Accepted: 29 March 2021 / Published online: 13 April 2021
© The Author(s) 2021

Abstract

The formation and development of faults are a manifestation of stress concentrations and energy release in crustal rocks, and faults have a great influence on the occurrence of dynamic mine disasters. This study proposed mapping technology as a fault identification method. The mapping procedure included four steps: (1) Drawing points on topographic maps. The information of topographic maps, such as elevation, rivers, and lakes was copied onto sulfuric acid paper. (2) Classifying the landform. Based on the highest and lowest points in the studied area, the minimum elevation difference was calculated and the elevation points were graded according to the minimum elevation difference. (3) Determining the block boundaries. The elevation points in the same grade were categorized into the same blocks. (4) Mapping the fault distribution. The boundaries between different blocks were considered as faults. In this regard, numbers were assigned to the faults, and a graphic scale, coordinate grid, and legends were added to the map. Fault identification for classes I–V was conducted at different scales. Fault identification for the next class always retained the previous results. Using this method, the faults in the Pingdingshan coal mining zone were divided into classes I–V. By comparing the classes with historical coal and gas outbursts, it was indicated that more than 90% of the coal and gas outbursts occurred in the vicinity of faults, especially at the intersections of multiple faults and in areas with concentrated faults. This study provided a scientific basis for predicting coal and gas outbursts.

Keywords Fault identification · Mapping technology · Topography · Coal and gas outburst

Introduction

Coal and gas outbursts represent a severe hazard in coal mines. They often cause casualties and equipment damages

to coal mining enterprises, reducing mining safety and economic efficiency. Outbursts occur because of the combined effects of ground stress, gas, and compatible physical and mechanical properties of coal (Díaz Aguado and González 2007; Wold et al. 2008; Fu et al. 2008; Wang et al. 2009; Zhang 2009). Many scholars have conducted extensive research regarding the influencing factors of coal and gas outbursts, including gas contents (Dennis 2017), ground stress (Pan et al. 2020), and the crushing effect (Zhang et al. 2020). There are over dozens of factors that may influence outburst threat (Jacek 2011; Norbert 2012).

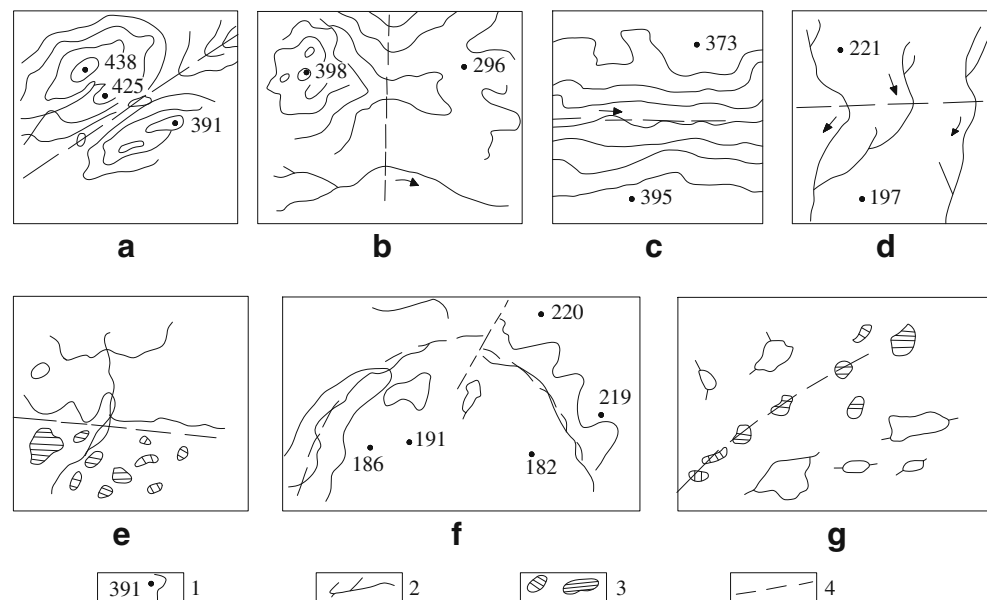
It is believed that most outbursts occur near geological structures (Jiang and Yu 1996; An et al. 2008; Han et al. 2008; Liu et al. 2010b; Liu et al. 2010b; Zhang et al. 2013). The geological structure in a mining zone determines the uneven distribution of coal and gas outbursts (Guo and Han 1998; Guo et al. 2002a, b). Farmer and Pooley (1967) found that all coal and gas outbursts occurred in regions that had experienced severe structural deformation, such as faults, folds, rolls, and slides, and in the tectonic coal development area. Shepherd et al. (1981) investigated the occurrences of

Responsible Editor: François Roure

✉ Ying Chen
56724647@qq.com

- ¹ Mining Engineering School, Liaoning Technical University, 47 Zhonghua Road, Fuxin 123000, Liaoning, China
- ² Research Center of Coal Resource Safe Mining and Clean Utilization, LNTU, Fuxin 123000, China
- ³ Engineering Laboratory of Deep Mine Rockburst Disaster Assessment, Jinan 250104, China
- ⁴ Shandong Energy Group Co., LTD, Jinan 250014, China
- ⁵ Shandong Provincial Research Institute of Coal Geology Planning and Exploration, Jinan 250104, China
- ⁶ Geophysical Survey Team of Shandong Coalfield Geology Bureau, Jinan 250104, China

Fig. 1 Geomorphic manifestations of faults: (1) elevation contours, (2) river, (3) lake, and (4) faults that form geomorphic features



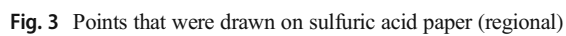
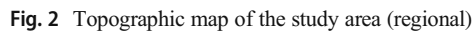
1) elevation contours, 2) river, 3) lake, 4) faults that form geomorphic features

coal and gas outbursts in Australia, Canada, the UK, France, and Poland. It was found that more than 90% of typical outbursts occurred in areas of strong deformation, such as the hinges of asymmetric anticlines, the hub area of plunging fold, strike-slip faults, nappe faults, and strong deformation zones around reverse and normal faults. Lama and Bodziony (1998) believed that folds, joints, faults, tectonic coal, variations in coal seam thickness, and magmatic intrusions affect coal and gas outbursts. Cai and Wang (2004) systematically summarized the coal and gas outbursts from 106 coal mines in 15 coalfields in China. Among 3082 accurately recorded outbursts, 2525 (81.9%) of them occurred in locations with geological structures, such as faults, folds, magmatic intrusions, and variations in coal seam thickness. Only 557 (18.1%) of the outbursts took place in areas without geological structures. Moreover, outbursts occurred in eight out of nine currently producing mines in Huainan, and 72 out of 129 outbursts (55.81%) were related to geological structures. Therefore, it could be concluded that the geological structure has a significant impact on the occurrence of coal and gas outbursts.

The results of the geological studies of outburst emphasizing structural conditions and tectonic stress field demonstrate that the outbursts are related to four factors: the structural characteristics, tectonic stress field, tectonic coal, and coal seam gas (Guo et al. 2002b; Zhang and Zhang 2005; Han et al. 2007; Liu et al. 2010a, b; Gao et al. 2012). In a study of tectonic stress, Zhu (1994) confirmed that the stress field adjacent to faults has a significant effect on outbursts. Han et al. (2011) discussed the effect of tectonic depressions on outbursts. Hao et al. (2012) analyzed the characteristics of tectonic stress caused by sliding at the locations of outbursts. Based on the geo-dynamic division theory, earthquakes, rockbursts, and coal and gas outbursts are associated with the movement and development of fault structures and are the result of the secondary formation of faults and fractures (Zhang 1998; Zhang et al. 2009). As the scale of the current plate tectonics is large, it cannot be applied directly to solve the dynamic hazard problems in a coal mine. Hence, the methods that can identify and detect faults in regional and local scales are needed. Such methods are applicable to engineering activities which are highly required.

Table 1 Empirical values of the minimum elevation difference (Δh_{\min}) used in the mapping

Fault classes	Topographic map scale	Minimum elevation difference/ Δh_{\min}
I	1:2,500,000	500m
II	1:1,000,000	200m
III	1:200,000	100m
IV	1:50,000	20–50m
V	1:10,000	5–10m



So far, many scholars have conducted a lot of research on fault identification and detection methods, including Landsat synthetic stereo pair (Salvi 1995), grid-based ensemble Kalman filter (Sun 2011), Alpha track (LR-115 type II) detectors (Asumadu-Sakyi et al. 2011), curvature (Zheng et al. 2014), diagnostic plots with the divergence time (Vilarrasa et al. 2017), seismic and scattered data analysis (Landa and Gurevich 1998; Xu et al. 2015; Noori et al. 2019), integration of remote sensing and geographic information systems (Mohamed and Alshamsi 2019), horizontal to vertical spectral ratio (HVSr) (Khalili and Mirzakardeh 2019), high-precision gravity data analysis (Zou et al. 2019), the mineral and bulk-rock compositions (Masakazu et al. 2019), temperature vegetation dryness index (Wang et al. 2019), and the multidisciplinary studies (e.g., archaeoseismology, remote sensing and geomorphology, surface geology and structural data, 2D resistivity imaging, and palaeoseismological trenching) (Similox-Tohon et al. 2006).

Based on the principle of geo-dynamic division (Chen et al. 2016), a fault identification method predominantly based on mapping technology was proposed in this study. The fault division by mapping was mostly based on the geomorphic characteristics of active faults. It had the feature of high efficiency, low cost, and easy operation. The procedure consisted of drawing points on a topographic map, classifying the landform, determining the block boundaries, and mapping the fault distribution. The faults were divided into classes I–V in the coal mine region. The fault's effect on coal and gas outbursts was also analyzed, which provided a scientific basis for predictions of dynamic disasters in coal mines.

A division method for faults

Geomorphic indicators of fault

Tectonic movement is the driving force for the formation and development of the earth's topography and geomorphology.

Table 2 Geomorphic elevation classification results

Elevation class	Elevation scope/m
1	240–260
2	260–280
3	280–300
4	300–320
5	320–340
6	340–360
7	360–380
8	380–400
9	400–420
10	420–440

Faults are consequences and indicators of crustal movement. Geomorphology reflects great information about faults. The geomorphic manifestation caused by faults can be divided into two categories. The first category is large-scale landform or macro-landform, which is the result of long-term effects of faults. The second one is the micro-landform, which is caused by a small number of abrupt events (such as earthquakes). The study of the geomorphic manifestations of the faults is important for understanding the characteristics and activity of faults.

The topography is sensitive to faults that can be identified from the earth's surface. Fault identification is a process of determination of the boundaries between blocks that are geodynamically related. Although the boundaries may become ambiguous due to erosion, the fault indicators are still visible. Faults can be identified by several topographic indicators, such as fault scarps and toe lines, bending of continuous river valleys, and beaded lakes (Fig. 1).

Fault identification method

Mapping is one of the major methods used to identify faults and is mainly conducted based on the geomorphic characteristics of faults. Based on the assumption that the basic forms and main characteristics of the topography and geomorphology depend on the geological structure, the formation and development of regional faults can be identified through topographic and geomorphic analyses. The fault identification principle is applied from a general to an individual perspective. Starting with the plate tectonics, by identification and division of classes I–V faults, the scope could be narrowed down to mine field scale, which linked plate tectonics with engineering applications. The mapping was conducted based on topographic maps. Topographic maps depicted three-dimensional characteristics of landform and provided evidence for analyzing landform origin. The mapping procedure included the following steps:

(1) Drawing points on topographic maps. The fault identification for different classes must be conducted on topographic maps with different scales (Table 1). After selecting the topographic map (e.g., division of class V faults at a scale of 1:10,000, as shown in Fig. 2), the topographic map was covered with a piece of transparent sulfuric acid paper. The elevation points whose locations and values were known on the topographic map were copied to the sulfuric acid paper. Rivers and lakes must also be mapped on the sulfuric acid paper. Thus, the topographic and geomorphic information primarily consisted of drawing the elevation points (Fig. 3).

(2) Classifying landform. The adjacent areas may be divided into different blocks by considering different elevations. For each region, the minimum elevation difference Δh_{\min} could be calculated using the following equation:

$$\Delta h_{\min} = 0.1 (H_{\max} - H_{\min}) \quad (1)$$

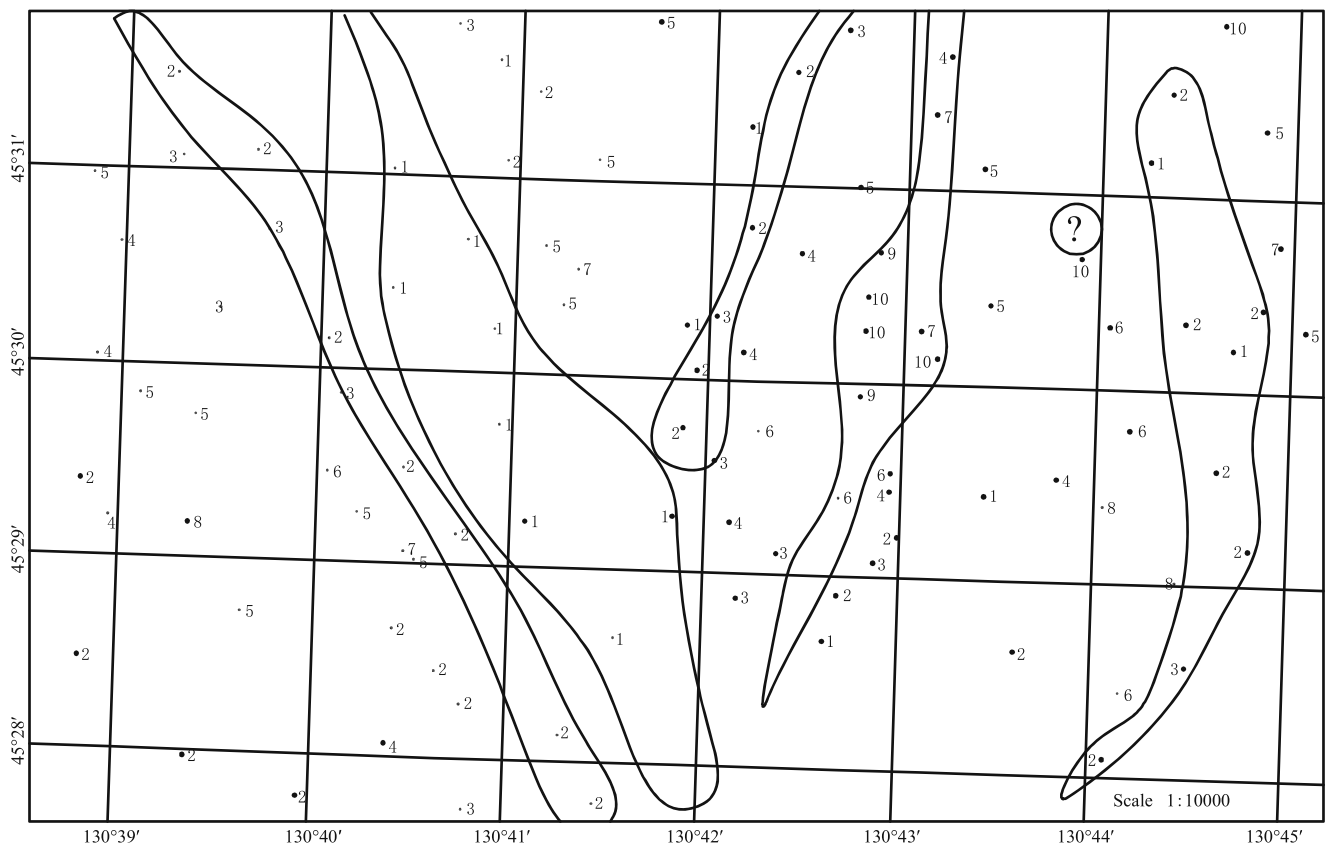


Fig. 4 Block division (partial)

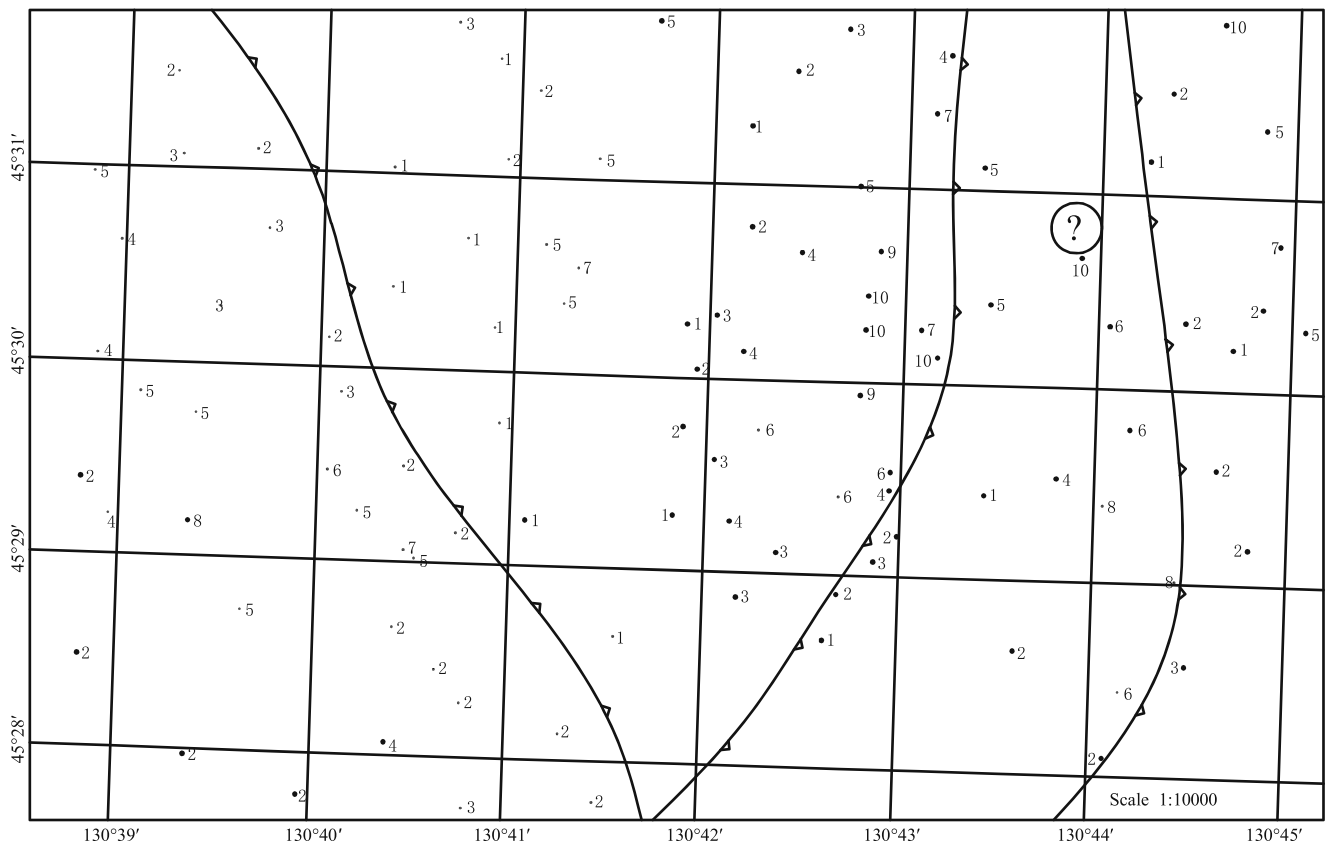


Fig. 5 Fault distributions (partial)

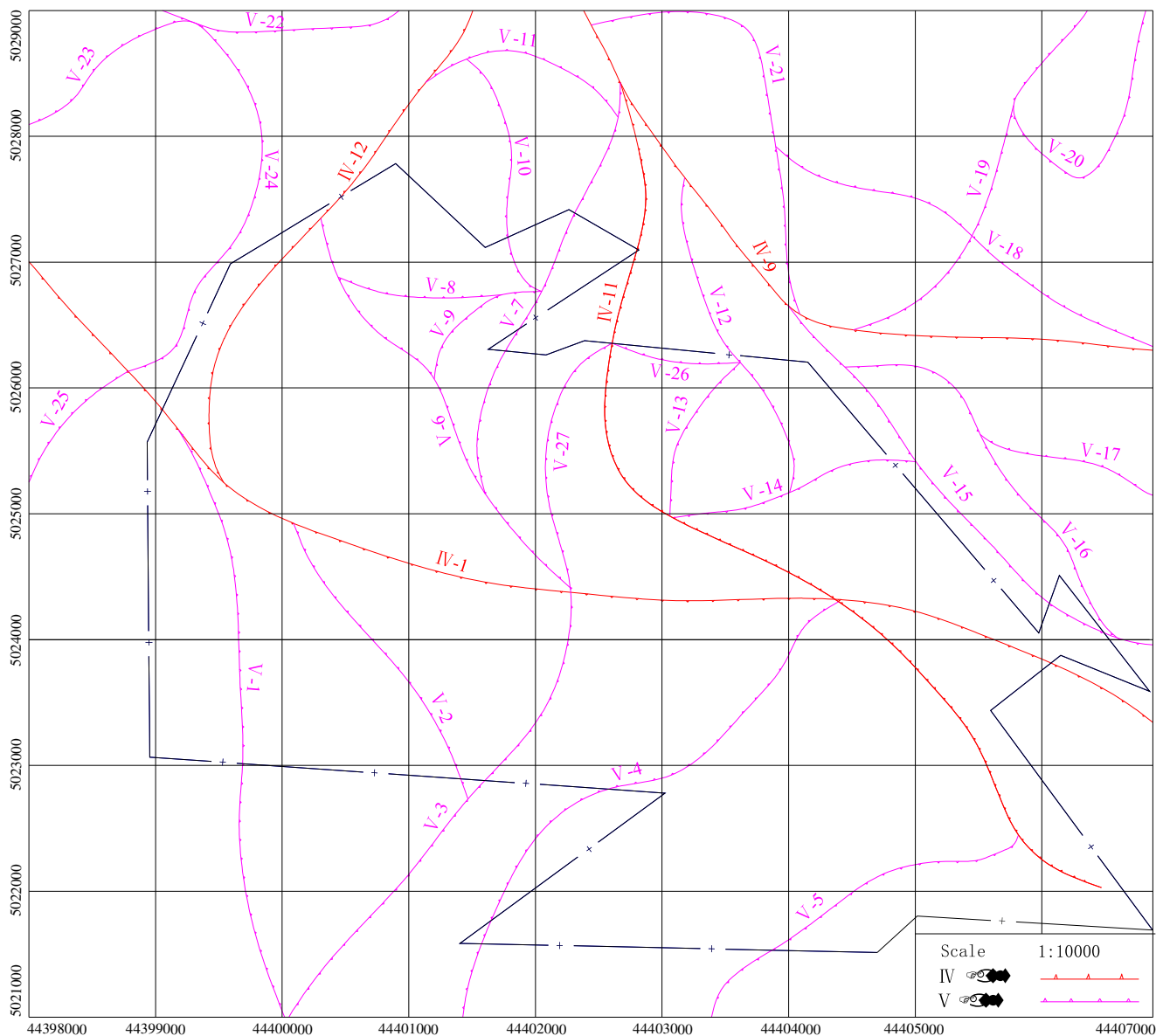


Fig. 6 Class V faults map

where H_{\max} is the maximum absolute elevation of the surface in the studied area (m) and H_{\min} is the minimum absolute elevation of the surface in the studied area (m).

Table 1 presents the empirical values of Δh_{\min} for the identification of classes I–V faults.

Based on Fig. 3, the highest and lowest points in the study area were determined. The maximum elevation was 439.4 m, and the minimum elevation was 241.5 m. Then, Δh_{\min} was calculated using Eq. (1) as follows:

$$\Delta h_{\min} = 0.1 \times (439.4 - 241.5) = 19.8 \text{ m} \quad (2)$$

Based on the result, the elevation points were divided into 10 classes with an interval of 20 m, and each class was labeled with numbers 1–10. The 10 geomorphic classes are presented in Table 2.

Based on Table 2, the elevation points in Fig. 3 were re-drawn using classes 1–10. The elevation points in one identical or similar class were drawn for one block. The studied area was divided into several blocks. Figure 4 illustrates part of the classified elevation points. We might encounter anomalous elevation points during the division process. For example, the elevation point of class “10” in the upper right part of Fig. 4 was surrounded by other elevation points of classes 5 and 6. Therefore, this point could be erroneous. The reason for this problem might be a human activity, such as a waste dump. These anomalous points must be corrected through a field survey.

(3) Determining the block boundaries. The block boundaries were determined based on the classification of elevation points. The boundaries between different blocks were faults.

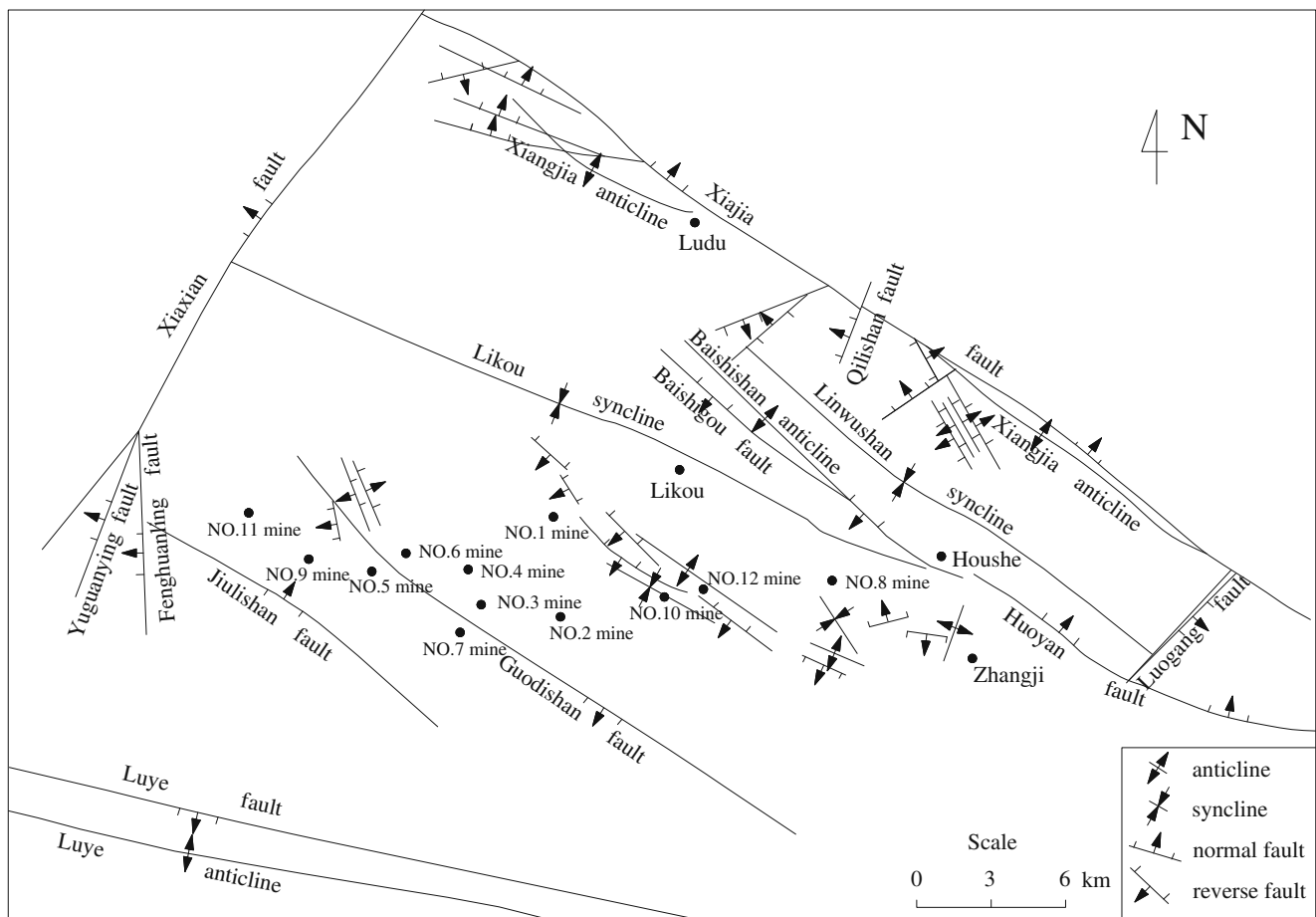


Fig. 7 Geological structures in Pingdingshan mining area

Fig. 8 Class I fault distribution in Pingdingshan mining area

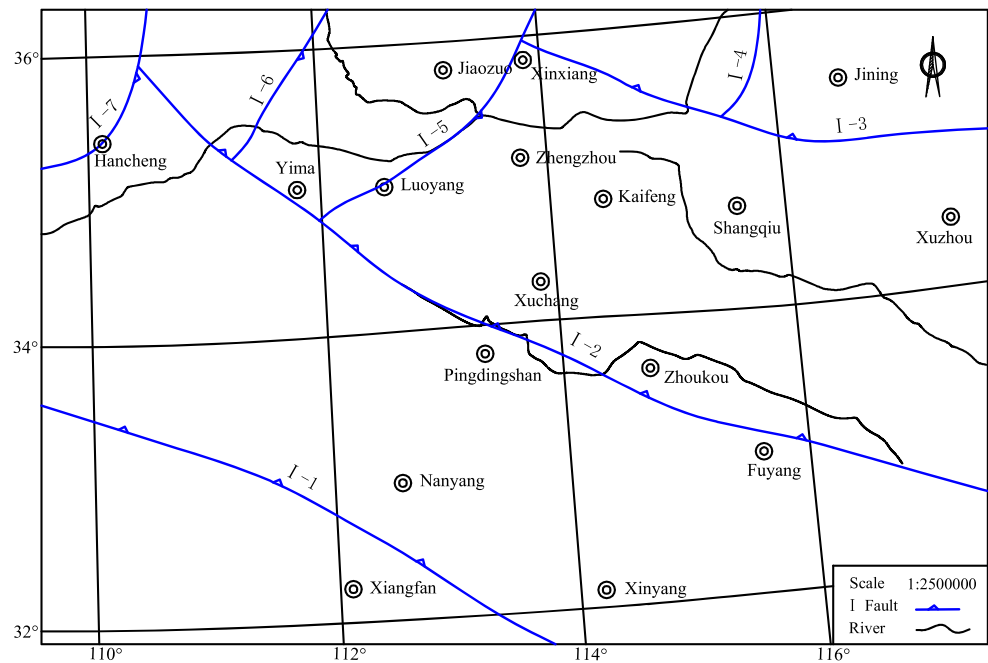


Table 3 Features of class I faults

Fault name	Orientation	Relationship to known fault	Landform	Movement type	Activity
I-1	294° - 303°	Liangyun Fault	Uplift	Strike-slip fault	
I-2	319° - 288°	Xin'an-Luye Fault			
I-3	292° - 87°	Xinxiang-Shangqiu Fault	Terrace	Dextral normal fault	Strong
I-4	11° - 48°	Liaocheng-Lankao Fault	Depression		Strong
I-5	32° - 69°	Tangxi Fault		Dextral-transform normal fault	Strong
I-6	33°	Taigu Fault			
I-7	15° - 79°	Hancheng-Huaxian Fault			

To identify faults, we also needed to analyze topographic and geomorphic features, such as fault scarps, linearly distributed beaded lakes, river bends, seismic data, and remote sensing images. The anomalous elevation point was modified through a field survey. Figure 5 exhibits the faults that were identified based on Fig. 4.

(4) Finishing fault distribution map. Roman and Arabic numbers were utilized to indicate fault class and number. For example, V-3 represents the third fault in class V. After adding a graphical scale, coordinate grid, and legend into the map, the fault distribution map was completed (Fig. 6).

Classes I–V faults could be identified by conducting the above process on topographic maps with different scales. Fault identification for the next class always retained previous results. For example, the identification of class V faults retained the results of classes I, II, III, and IV. Class V faults narrow the scope of a coal mine, which can be used for engineering activities.

Fault identification application and its impact on coal and gas outbursts in Pingdingshan mining area

Fault identification in Pingdingshan mining area

The Pingdingshan mining area is characterized by a belt of block uplifts and circumferential depressions. It is bounded by the Jiaxian normal fault, the Xiangjia normal fault, and the Yelu normal fault (Fig. 7). The main structure is the Likou syncline that is a broad and gentle synclinorium. The axis of the syncline trends 300–310° and plunges to the northwest. The dip angles of the two wings are 5–15°.

Identification of class I faults

Eight class I faults were identified on a 1:2,500,000-scale topographic map using the mapping method (Fig. 8). The

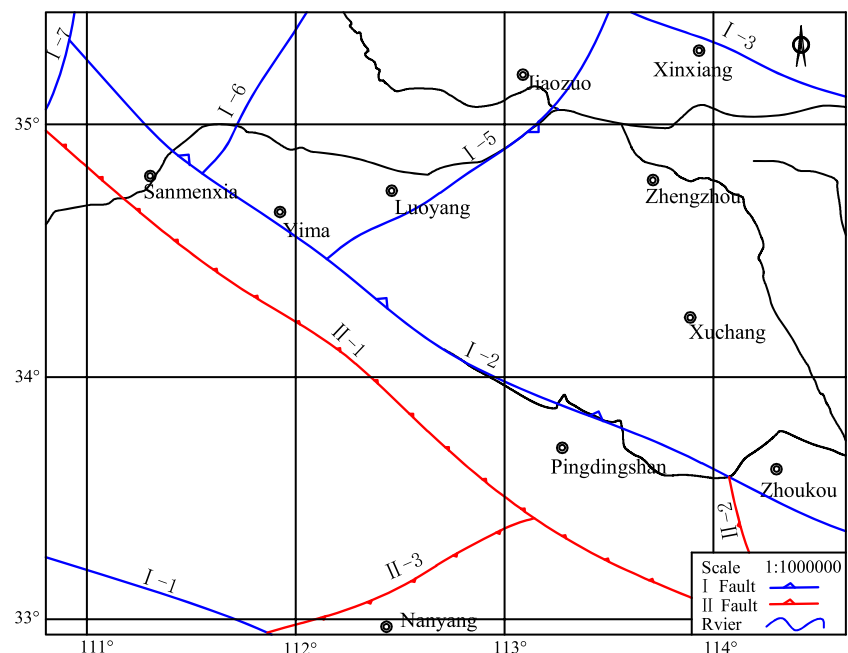
Fig. 9 Class II fault distribution in Pingdingshan mining area

Table 4 Features of class II faults

Fault name	Orientation	Relationship to known fault	Geomorphology	Movement type	Activity
II-1	311° - 295°	Checun-Lushan Fault	A chain of beaded lakes, terraces	Dextral	
II-2	345°		A chain of beaded reservoirs, elevation differences		
II-3	63° - 72°		Terraces		

results indicated not only numerous known faults but also several new faults. The features of the class I faults are presented in Table 3.

The class I faults were located within the Hehuai block of the North China plate. Fault I-1 is related to Liangyun Fault (Yunxian-Yunxi Fault) which is an important fault in the central orogenic zone. It has undergone a significant strike-slip deformation since the Quaternary. Fault I-2 is related to the known Xin'an Fault and Luye Fault, but its end is newly developed. Fault I-3 is related to the Xinxiang-Shangqiu Fault that is the boundary between the Jilu block and the Yuwan block. It crosses the northern downtown area of Shangqiu city and causes strong earthquakes. Fault I-4 is related to Liaocheng-Lankao Fault that is located on the Huabei platform. As the boundary of the Huabei fault zone and Luxi fault zone, it controls the formation of tectonic patterns in neighbor areas. Fault I-5 is related to the Tangxi Fault that is a dextral-transform normal fault. It experienced intense activity in Neogene. Fault I-6 is the Taigu Fault, and fault I-7 is the Hancheng-Huaxian Fault.

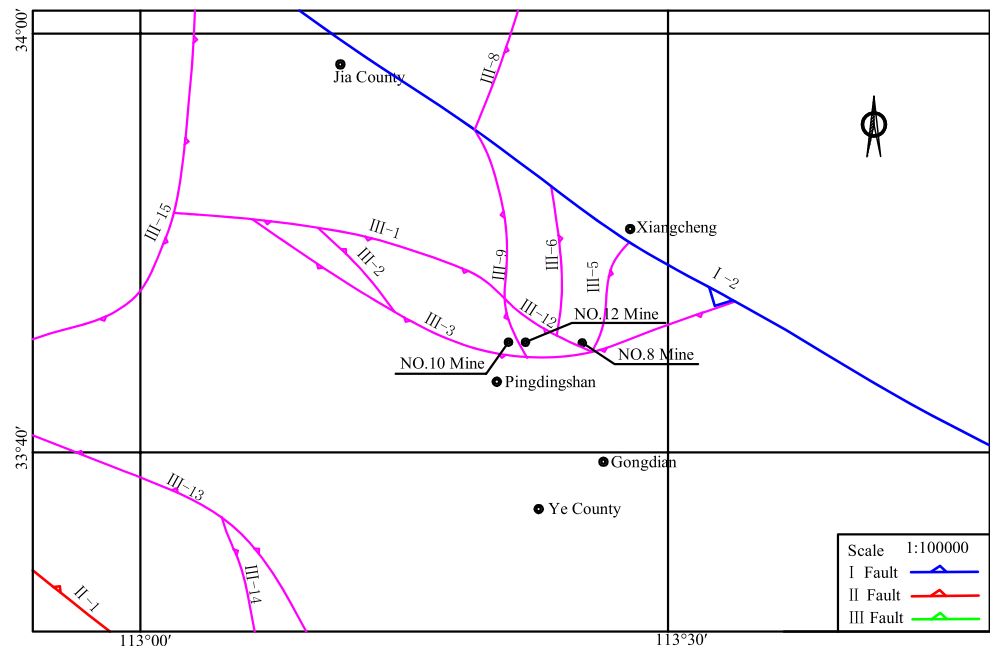
Identification of class II faults

Three class II faults were identified on a 1:1,000,000-scale topographic map through the mapping method (Fig. 9). The features of the class II faults are presented in Table 4.

Fault II-1 is related to the Checun-Lushan Fault and is marked by a chain of beaded lakes and boundaries between highlands and lowlands. It extends several hundred kilometers from northeast to southwest. Fault II-2 strikes northwest. The elevation difference of its both sides reaches thousands of meters. Numerous linear small lakes and reservoirs distribute along this fault. Fault II-3 intersects with fault II-1 at Suya Lake.

Identification of classes III, IV, and V faults

Classes III, IV, and V faults were identified on topographic maps of Pingdingshan East Mining area as a center with scales of 1:100,000, 1:50,000, and 1:10,000, respectively. Overall, there were 15 class III faults, 11 class IV faults, and 31 class V faults that needed to be identified. Details of these faults are shown in Figs. 10, 11, and 12, respectively.

Fig. 10 Class III fault distribution in Pingdingshan mining area

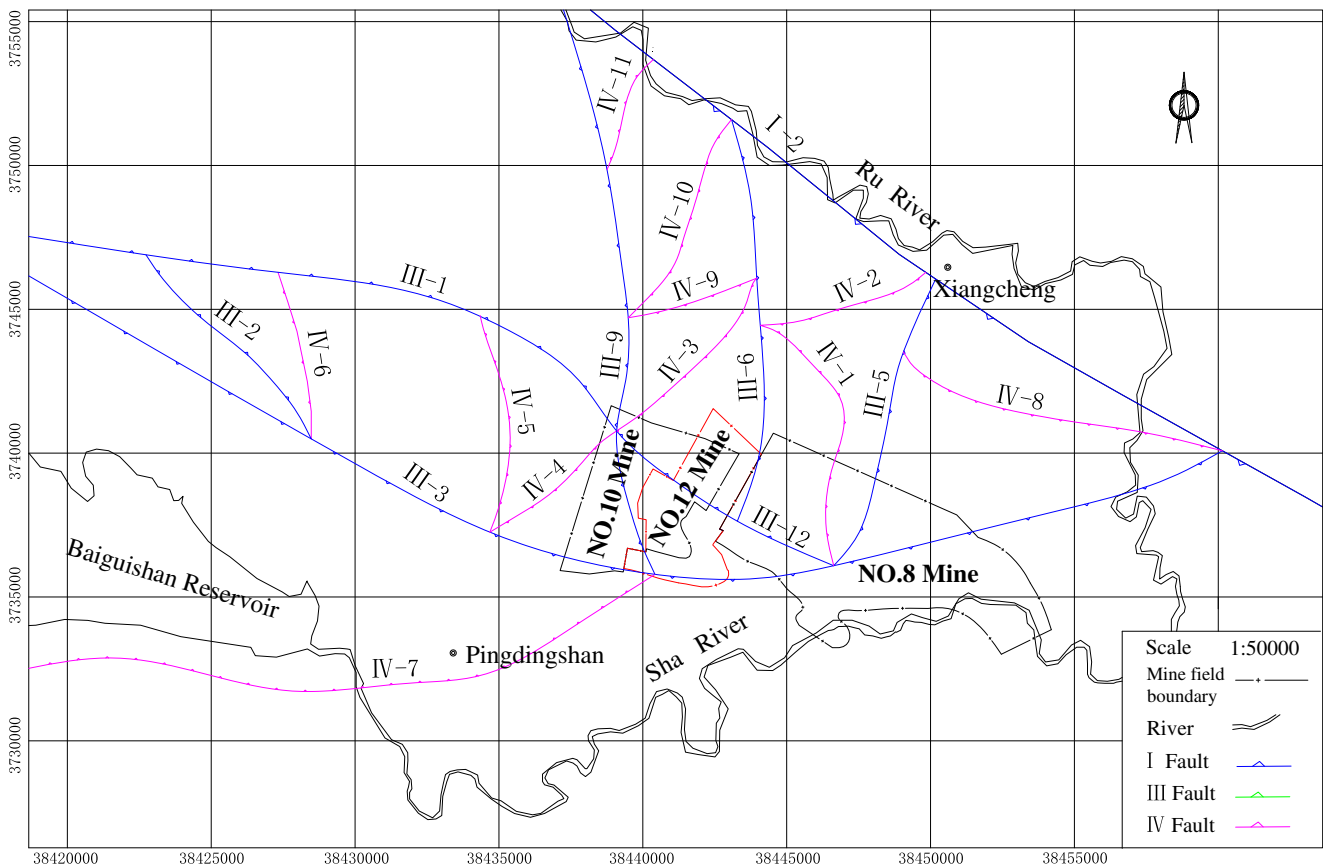


Fig. 11 Class IV fault distribution in Pingdingshan mining area

Effect of faults on coal and gas outbursts

Effect of faults on No. 8 mine coal and gas outbursts

Coal and gas outbursts in the western part of the No. 8 mine were largely affected by faults III-6, III-12, V-1, V-2, V-11, and V-12 (Fig. 13). The E₉₋₁₀ coal seam had experienced 24 coal and gas outburst events, 19 of which (79.2%) occurred between faults III-12 and V-1.

The coal and gas outbursts in the eastern part of the No. 8 mine were chiefly affected by faults III-3, III-5, and V-9. The F₁₅ coal seam had experienced 18 coal and gas outbursts, 15 of which (83.3%) took place at the intersection of faults III-3, III-5, and V-9 and were distributed on both sides of fault III-3.

Effect of faults on No. 10 mine coal and gas outbursts

Coal and gas outbursts that occurred in the No. 10 mine were concentrated on the north of fault III-12 and were affected by several class V faults, including faults V-12, V-13, and V-24 (Fig. 14). The E₉₋₁₀ coal seam had experienced 33 coal and gas outbursts, 24 of which (84.0%) occurred near fault V-12

and between faults V-12 and V-13. Two of them (8.0%) took place at the intersection of faults V-13, V-23, and V-24, four of them (16%) happened near the intersections of faults III-1, III-9, III-12, IV-3, and IV-4, and one of them (4%) occurred near fault V-28. The area surrounded by faults III-12, V-12, V-13, V-24, and V-25 was an area with a high rate of occurrence of coal and gas outbursts. High-density faults cause severe rock fracturing and stress concentrations that are the main reason for high frequent and intense coal and gas outbursts.

Effect of faults on No. 12 mine coal and gas outbursts

Coal and gas outbursts that occurred in the No. 12 mine were concentrated at the intersection of faults III-9 and V-11 and in the area surrounded by faults III-12 and V-13 (Fig. 15). The No. 12 mine had experienced 31 coal and gas outbursts. Twenty of them (64.5%) occurred near the intersection of faults III-9 and V-11, nine of them (29.0%) took place within the area that was surrounded by faults III-12 and V-13, and two of them happened near fault V-14.

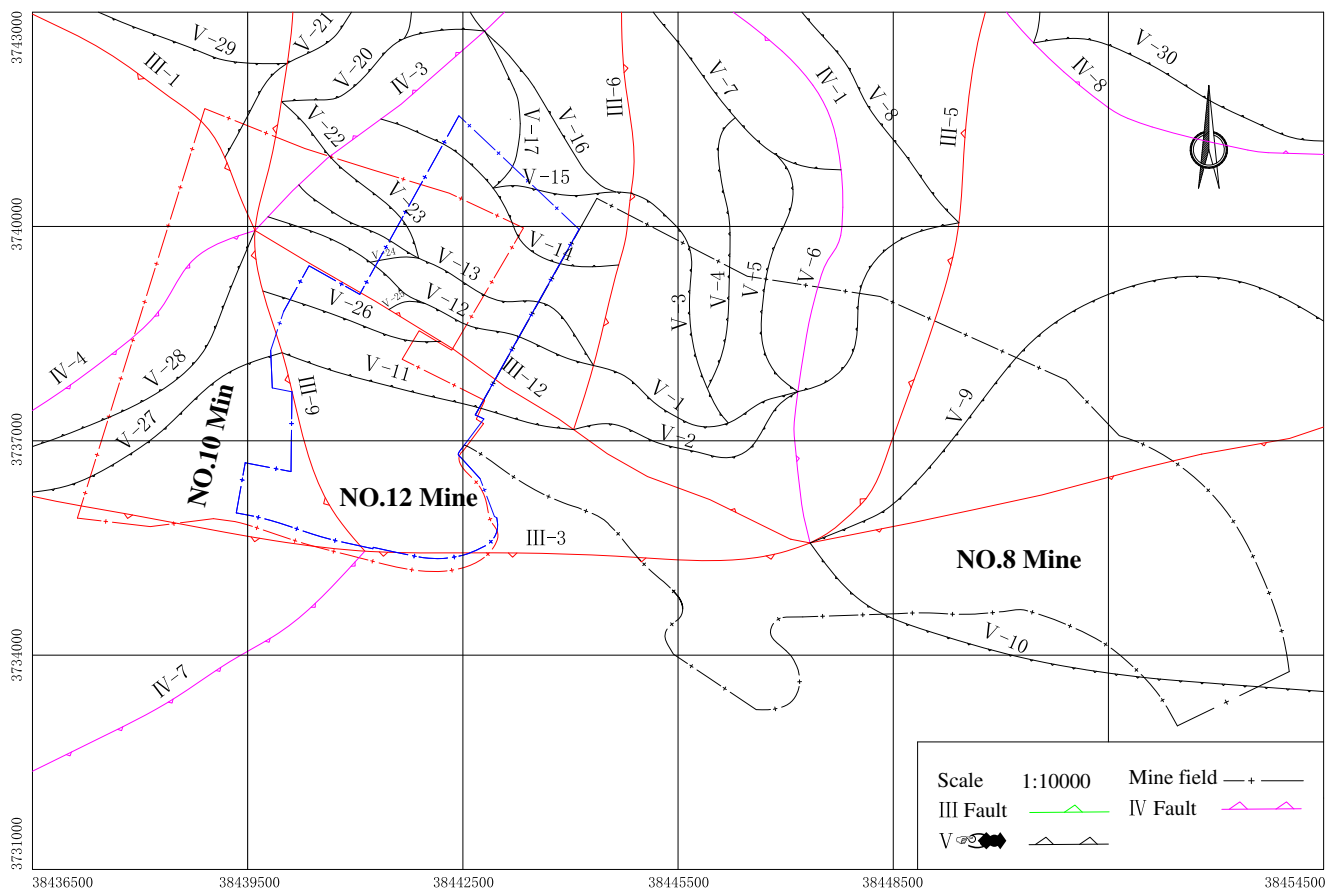


Fig. 12 Class V fault distribution in Pingdingshan mining area

Coal and gas outbursts often occurred near faults. The analysis demonstrated that more than 90% of the coal and gas outbursts that had occurred at Pingdingshan No. 8, No. 10, and No. 12 mines were closely related to the mapped faults. The intersections of multiple faults and areas with high-density faults were also prone to coal and gas outbursts.

Discussion

A practical project showed that coal and gas outbursts were more likely to occur in areas where faults were dense or multiple faults intersected. The mapping was employed to determine the distribution of faults suitable for mining engineering. According to the results, the risk of coal and gas outbursts in different areas could be predicted. Based on this, it becomes possible to optimize the mining layout rationally or to take preventive measures before mining in a high-risk region. It provides a guarantee for safe

mining. It also has a great significance for the prediction and prevention of coal and gas outbursts.

Dividing the active faults by the use of mapping will produce uncertainty. Natural erosion, weathering, or artificial transformation will change the original topography and landforms, which causes errors in the division results. Therefore, it is necessary to modify and verify the results in combination with other methods. Field survey is an important method. The mission of the field survey includes geomorphological elevation point inspection, fault geomorphological fragment survey, water system analysis, river terrace deformation, river capture and rerouting, building survey, and geophysical exploration of fault on the ground and underground. Meanwhile, researchers can check the facts through an aerial photograph or by using geographical information systems. Besides, based on the exposure in actual mining activities, the fault division can be further revised and improved.

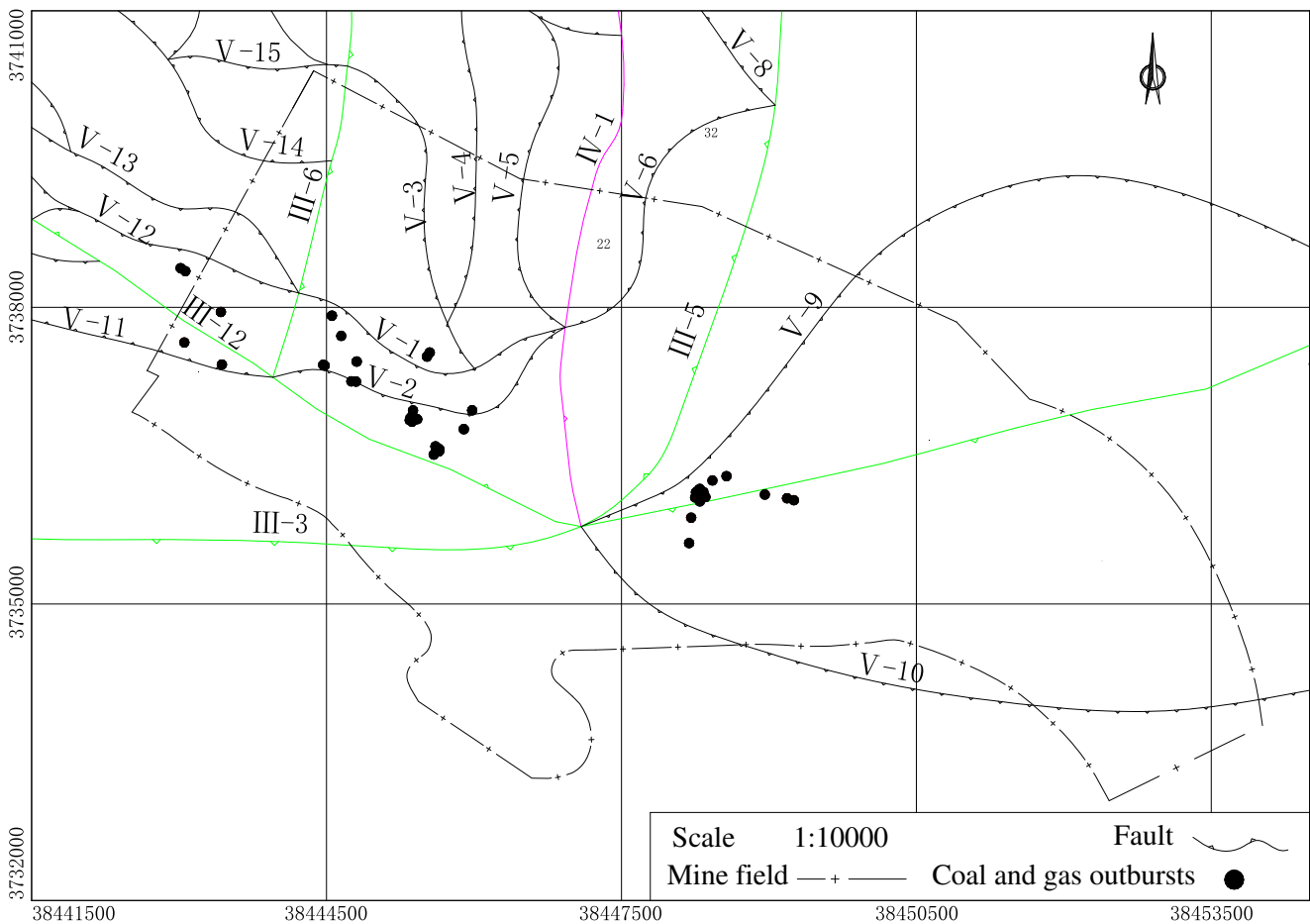


Fig. 13 Relationship between coal and gas outbursts and faults in the No. 8 mine

The fault has obvious control and influence on coal and gas outbursts closely related to mining activities. This is an accepted opinion of many scholars. This study was based on a fault identification approach using mapping. In this regard, the relationship between the fault distribution and coal and gas outbursts was established in combination with actual engineering conditions. This relationship can be utilized to predict and prevent coal and gas outbursts in mines. The stress change during fault formation and development and fault activity and mining activities influencing coal and gas outburst have not been analyzed yet. We plan to discuss these issues in subsequent research.

Conclusion

The following main conclusions were drawn from this study:

- (1) The formation and development of faults are an indicator of crustal movements and a manifestation of stress concentrations and energy release in crustal rocks. Faults can be identified and categorized by their topographic and

geomorphic characteristics. Based on topography, this study proposed mapping technology as a fault identification method.

- (2) The mapping procedure included drawing points on a topographic map, classifying landform, determining block boundaries, and completing the fault distribution map. The mapping process followed the general-to-individual principle. Faults were identified and divided into class I to V with different scales. Finally, fault distribution suiting a mine scale was determined. It established the relationship between plate tectonics and engineering applications.
- (3) Using the proposed mapping technology, the faults in the Pingdingshan mining area were divided into classes I–V. By comparing the fault distribution with the site of coal and gas outbursts in the mines, the results demonstrated that more than 90% of coal and gas outbursts were affected by faults. The intersections of multiple faults and areas with concentrated faults were prone to coal and gas outbursts.
- (4) The mapping established the connection between the faults and coal and the gas outbursts. Based on this

Fig. 14 Relationship between coal and gas outbursts and faults in the No. 10 mine

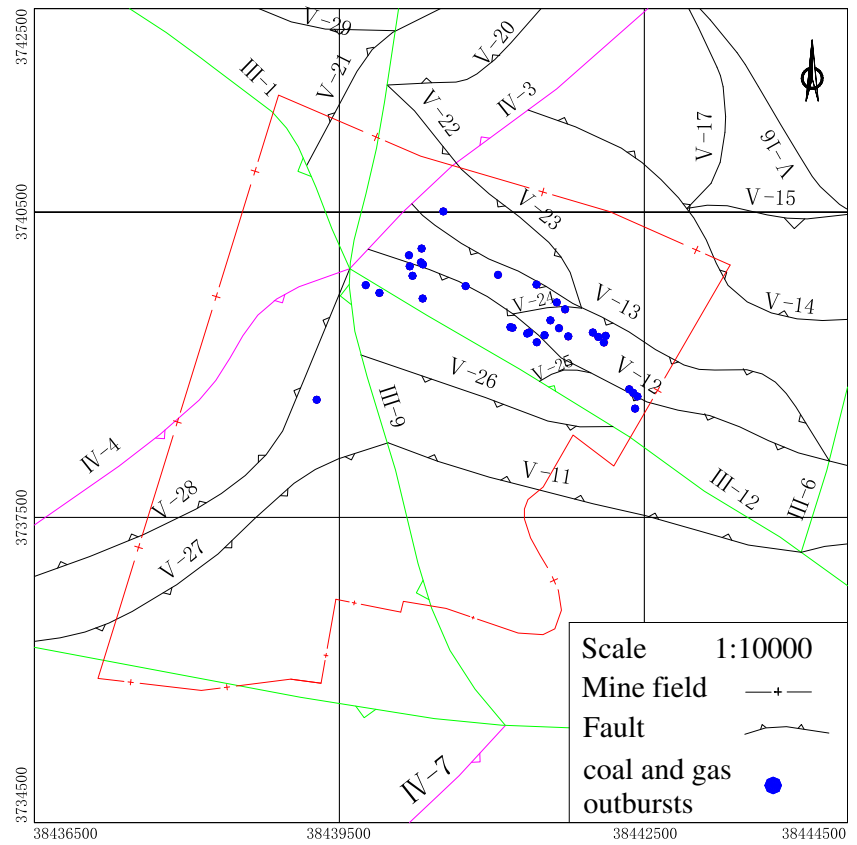
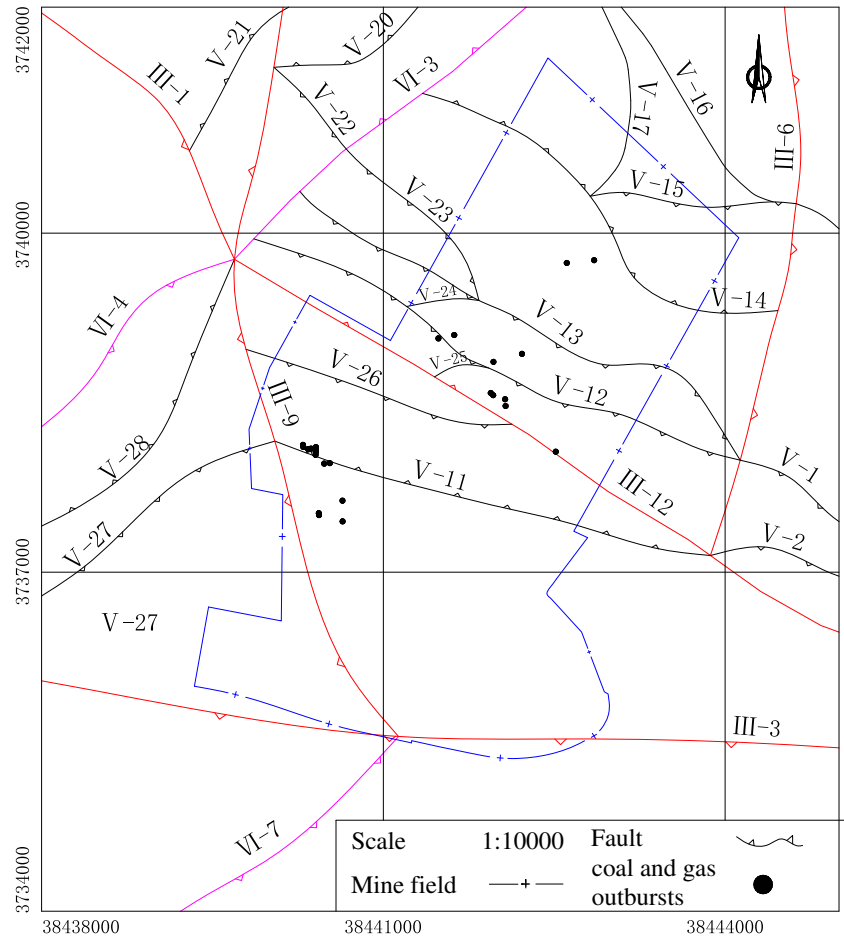


Fig. 15 Relationship between coal and gas outbursts and faults in the No. 12 mine



connection, mining engineers can apply controlling measures in high incidence areas to prevent coal and gas outbursts, which is significant for mining safety. This study also provided a scientific basis for predicting coal and gas outbursts.

Acknowledgements Special thanks to Fengjun Hou and Yunlong Wu for their help in the site work. We are also grateful to EditSprings (<https://www.editsprings.com/>) for the expert linguistic services provided.

Funding This study was financially supported by the National Natural Science Foundation of China (Grant No. 51874164, No. 51704148, and No. 51674135), National Key R&D Program of China (Grant No. 2017YFC0804203), Open Projects of Engineering Laboratory of Deep Mine Rockburst Disaster Assessment (Grant No. (2020)011), and Major scientific and technological innovation projects in Shandong Province (Grant No. 2019SDZY02).

Declarations

Conflict of interest The authors declare that they have no competing interests.

Open Access This article is licensed under a Creative Commons Attribution 4.0 International License, which permits use, sharing, adaptation, distribution and reproduction in any medium or format, as long as you give appropriate credit to the original author(s) and the source, provide a link to the Creative Commons licence, and indicate if changes were made. The images or other third party material in this article are included in the article's Creative Commons licence, unless indicated otherwise in a credit line to the material. If material is not included in the article's Creative Commons licence and your intended use is not permitted by statutory regulation or exceeds the permitted use, you will need to obtain permission directly from the copyright holder. To view a copy of this licence, visit <http://creativecommons.org/licenses/by/4.0/>.

References

- An HT, Sun SQ, Chen ZS, Zhao JZ (2008) Geological conditions affected to coal and gas outburst in Daxing Mine. *Coal Sci Technol* 36(9): 47–49 (in Chinese)
- Asumadu-Sakyi AB, Fletcher JJ, Oppon OC et al (2011) Preliminary studies on geological fault location using solid state nuclear track detection. *Res J Environ Earth Sci* 3(1):24–31
- Cai C-g, Wang Y (2004) Qualitative and quantitative analysis of general regularity of coal and gas outburst. *China Safety Sci J* 14(6):109–112 (in Chinese)
- Chen Y, Hongwei Z, Yu B, Zhu Z, Wu W, Yunpeng L (2016) Study of influence of regional geodynamic background on strata behaviors in China's Tongxin mine. *Resour Geol* 66(1):1–11
- Dennis JB (2017) Investigations into the identification and control of outburst risk in Australian underground coal mines. *Int J Min Sci Technol* 27(05):749–753
- Díaz Aguado MB, González NC (2007) Control and prevention of gas outbursts in coal mines, Riosa-Olloniego coalfield, Spain. *Int J Coal Geol* 69(4):253–266
- Farmer IW, Pooley FD (1967) A hypothesis to explain the occurrence of outbursts in coal based on a study of West Wales outburst coal. *Int J Rock Mech Min Sci* 4:189–193
- Fu X, Wang KJ, Yang TH (2008) Gas irradiation feature of tectonic coal. *J China Coal Soc* 33(7):775–779 (in Chinese)
- Gao K, Liu ZG, Liu J (2012) Comprehensive analysis of geological structure physical environment impact on coal and gas outburst. *Safety Coal Mines* 43(8):174–176 (in Chinese)
- Guo DY, Han DX (1998) Research on the types of geological tectonic controlling coal-gas outbursts. *J China Coal Soc* 23(4):337–341 (in Chinese)
- Guo DY, Han DX, Wang XY (2002a) Outburst-prone tectonophysical environment and its applications. *J Univ Sci Technol Beijing* 24(6):581–584 (in Chinese)
- Guo DY, Han DX, Zhang JG (2002b) Research on the occurrence and distribution of structural coal in Pingdingshan coal district. *J China Coal Soc* 27(3):249–253 (in Chinese)
- Han J., Zhang H.W., Zhu Z.M and Song J.C. (2007) Controlling of tectonic stress field evolution for coal and gas outburst in Fuxin bash. *J China Coal Soc*, 32(9):934–938. (in Chinese)
- Han J, Zhang HW, Huo BJ (2008) Discussion of coal and gas outburst mechanism of syncline. *J China Coal Soc* 33(8):908–913 (in Chinese)
- Han J, Zhang HW, Song WH, Li S, Lan TW (2011) Coal and gas outburst mechanism and risk analysis of tectonic concave. *J China Coal Soc* 36(Supp.1):108–113 (in Chinese)
- Hao FC, Liu MJ, Wei JP, Fu YQ (2012) The controlling role of gravitational slide structure to coal and gas outburst. *J China Coal Soc* 37(5):825–829 (in Chinese)
- Jacek S (2011) The influence of sorption processes on gas stresses leading to the coal and gas outburst in the laboratory conditions. *Fuel* 90(3): 1018–1023
- Jiang CL, Yu QX (1996) Rules of energy dissipation in coal and gas outburst. *J China Coal Soc* 21(2):173–178 (in Chinese)
- Khalili M, Mirzakerdeh AV (2019) Fault detection using microtremor data (HVSAR-based approach) and electrical resistivity survey. *J Rock Mech Geotech Eng* 11(2):400–408
- Lama RD, Bodziony J (1998) Management of outburst in underground coal mines. *Int J Coal Geol* 35:83–115
- Landa E, Gurevich B (1998) Interference pattern as a means of fault detection. *Lead Edge* 17(6):752–757
- Liu YW, Chen P, Wei JP (2010a) Seam geological structure to control role of coal and gas outburst. *Coal Sci Technol* 38(1):24–27 (in Chinese)
- Liu YQ, Yang J, Zhang YG (2010b) Simulation on coal and gas outburst with discontinuous deformation analysis method. *J China Coal Soc* 35(5):797–801 (in Chinese)
- Masakazu N, Shimada K, Ishimaru T, Tanaka Y (2019) Identification of capable faults using fault rock geochemical signatures: A case study from offset granitic bedrock on the Tsuruga Peninsula, central Japan. *Eng Geol* 260:1–15
- Mohamed E, Alshamsi D (2019) Integration of remote sensing and geographic information systems for geological fault detection on the island of Crete. *Greece* 8(1):45–54
- Noori M, Hassani H, Javaherian A, Amindavar H, Torabi S (2019) Automatic fault detection in seismic data using Gaussian process regression. *J Appl Geophys* 163:117–131
- Norbert S (2012) Laboratory study of the phenomenon of methane and coal outburst. *Int J Rock Mech Min Sci* 55(Complete):102–107
- Pan XK, Cheng H, Chen J et al (2020) An experimental study of the mechanism of coal and gas outbursts in the tectonic regions. *Eng Geol* 279(105883):1–12
- Salvi S (1995) Analysis and interpretation of Landsat synthetic stereo pair for the detection of active fault zones in the Abruzzi region (Central Italy). *Remote Sens Environ* 53(3):153–163
- Shepherd J, Rixon LK, Griffith L (1981) Outbursts and geological structures in coal mines, A Review. *Int J Rock Mech Min Sci* 18:268–283

- Similox-Tohon D, Sintubin M, Muchez P, Verhaert G, Vanneste K, Fernandez M, Vandycke S, Vanhaverbeke H, Waelkens M (2006) The identification of an active fault by a multidisciplinary study at the archaeological site of sagalassos (sw turkey). *Tectonophysics* 420(3–4):371–387
- Sun AY (2011) Identification of geologic fault network geometry by using a grid-based ensemble kalman filter. *J Hazard Toxic Radioact Waste* 15(4):228–233
- Villarrasa V, Bustarret G, Laloui L, Zeidouni M (2017) A methodology to detect and locate low-permeability faults to reduce the risk of inducing seismicity of fluid injection operations in deep saline formations. *Int J Greenhouse Gas Control* 59:110–122
- Wang JL, Jiang B, Chen F (2009) Controlling effect of the interaction of tectonic coal with stress field to coal-gas outburst. *Safety Coal Mines* 40(11):94–97 (in Chinese)
- Wang C, Chen J, Chen X, Chen J (2019) Identification of concealed faults in a grassland area in Inner Mongolia, China, using the temperature vegetation dryness index. *J Earth Sci* 30(4):853–860
- Wold MB, Connell LD, Choi SK (2008) The role of spatial variability in coal seam parameters on gas outburst behaviour during coal mining. *Int J Coal Geol* 75(1):1–14
- Xu HQ, Sun SZ, Gui ZX, Luo SL (2015) Detection of sub-seismic fault footprint from signal-to-noise ratio based on wavelet modulus maximum in the tight reservoir. *J Appl Geophys* 114:259–262
- Zhang HW (1998) Study of active faults and forecast of dynamic phenomena in mines. *J China Coal Soc* 23:113–117 (in Chinese)
- Zhang ZM (2009) Gas geology. China University of Mining and Technology Press, Xuzhou (in Chinese)
- Zhang ZM, Zhang YG (2005) Investigation into coal gas outburst occurred in Duping coal mine by using theories of gas geology. *J China Coal Soc* 30(2):137–140 (in Chinese)
- Zhang HW, Han J, Song WH (2009) Geodynamic division, vol 275. China Coal Industry Publishing House, Beijing (in Chinese)
- Zhang YY, Huang ZF, Yu GJ, Zhang HQ (2013) Coal and gas outbursts characteristics and countermeasures under the influence of geological conditions. *Coal Sci Technol* 41(12):39–45 (in Chinese)
- Zhang CL, Wang EY, Xu J et al (2020) A new method for coal and gas outburst prediction and prevention based on the fragmentation of ejected coal. *Fuel* 287(119493):1–10
- Zheng ZH, Tan JQ, Liu K (2014) Most extreme curvature and its application to seismic structural interpretation. *Appl Mech Mater* 522–524:1266–1269
- Zhu XS (1994) The controlling effect of tectonic stress field and its evolution on coal and gas outburst. *J China Coal Soc* 19(3):304–313 (in Chinese)
- Zou BL, Li TL, Wu YG, Wu HY, Shi JQ, Lin BZ (2019) Applications of gravity data in identification of faults and tectonic boundaries of a working area in Inner Mongolia. *Global Geol* 22(02):133–140